SCALABLE ELECTROSPRAY COMPONENTS FOR PORTABLE POWER APPLICATIONS USING MEMS FABRICATION TECHNIQUES

C. M. Waits, N. Jankowski*, and B. Geil
U.S. Army Research Laboratory, Adelphi, MD

ABSTRACT

Methods for integrative assembly and manufacturing using micro-electro mechanical systems (MEMS) fabrication are reported for a novel compact fuel injector having applications in soldier level power systems. MEMS techniques are used to precisely fabricate and accurately assemble the components of a multiplexed electrospray device allowing for higher compactness, while achieving higher flow rates and using lower power. Integrated devices are reported to achieve 20 cc/hour of ethanol flow with a droplet size of 11μm using a voltage of 1.8kV.

1. INTRODUCTION

Small scale portable power systems based on the combustion of liquid hydrocarbons has become of great interest in the last decade [Epstein et al. 1997, Groshenry 1995, Muler and Fréchette 2002, Fréchette et al. 2003, Walther and Pisano 2003, Knoblock et al. 2001, Kyritsis et al. 2002]. These combustion systems take advantage of the significantly higher energy density available in liquid hydrocarbons when compared to conventional batteries (at only 10% efficiency, diesel fuel can yield 5MJ/kg, 10 times more than the 0.5MJ/kg for primary batteries). Compact combustion devices in the cm^3 range will likely use catalytic conversion and diffusion controlled combustion requiring the fuel to be delivered as small and rapidly evaporating droplets [Deng et al. 2006].

Using a combination of manually assembled micromachined and conventionally machined components, researchers at Yale University demonstrated that multiplexed electrospray is an effective way to break up heavy hydrocarbon fuels into fine droplets [Deng et al. 2006]. They obtained flow rates in the 10's of cc/hour range using a density of 250 nozzles/cm^2. Other techniques that utilize electrospray technology have not succeeded in creating such a high density of nozzles and, therefore, have had very low flow rate capabilities [Bocanegra et al. 2006, Tang et al. 2001].

Further reduction in the size of the multiplexed electrospray developed by Deng et al. is currently restricted by the manual assembly technique of the components. Alignment accuracy of only 50μm prevents the assembly of smaller electrospray components than reported. Because droplet characteristics are not affected by the changes in nozzle dimensions, improved fabrication and assembly techniques can shrink the nozzle size and increase the nozzle density. Increased nozzle density would allow further increases in device flow rate capability while maintaining sub-10μm droplet diameters.

We report on micro-electro mechanical systems (MEMS) fabrication techniques to precisely fabricate and accurately assemble the components of the electrospray device, allowing for more compact devices with higher flow rates and lower operating voltage. We review the single electrospray and multiplexed electrospray techniques in section 2. Section 3 describes the fabrication and assembly of an integrated multiplexed electrospray and Section 4 discusses the operation of the integrated devices.

2. MULTIPLEXED ELECTROSPRAY

Electrospray is a phenomenon discovered in 1914 by Jack Zeleny [Zeleny 1914] in which the meniscus of a charged liquid formed at the end of a capillary tube can be broken up into fine droplets using an electric field. Figure 1 demonstrates this for a single capillary tube. The electric field induced between the electrode and the conducting liquid initially causes a Taylor cone to form at the tip of the tube where the field becomes concentrated. Coulomb interaction between neighboring liquid ions causes them to separate from one another while being pulled towards the electrode. The droplet diameter has a power law dependence on the flow rate of the fuel ($D \propto \dot{Q}^{0.5}$ for JP-8 diesel [Deng et al. 2006]) implying that the flow rate has to be decreased to reduce the droplet size. In portable power generation applications, this requirement correlates to a flow rate that is too small to be useful.

Multiplexed electrospray, on the contrary, consists of arraying the tubes or nozzles, thereby increasing the overall flow rate without affecting the size of the ejected droplets. In order to maximize the flow rate and miniaturize the entire system, MEMS fabrication techniques can be used to create densely packed nozzles in silicon and integrate them with the other components. Figure 2 depicts the multiplexed electrospray with a ring

Report Documentation Page

Form Approved
OMB No. 0704-0188

1. REPORT DATE	2. REPORT TYPE	3. DATES COVERED
01 NOV 2006	**N/A**	**-**

4. TITLE AND SUBTITLE	5a. CONTRACT NUMBER
Scalable Electrospray Components For Portable Power Applications Using Mems Fabrication Techniques	5b. GRANT NUMBER
	5c. PROGRAM ELEMENT NUMBER
6. AUTHOR(S)	5d. PROJECT NUMBER
	5e. TASK NUMBER
	5f. WORK UNIT NUMBER
7. PERFORMING ORGANIZATION NAME(S) AND ADDRESS(ES) **U.S. Army Research Laboratory, Adelphi, MD**	8. PERFORMING ORGANIZATION REPORT NUMBER
9. SPONSORING/MONITORING AGENCY NAME(S) AND ADDRESS(ES)	10. SPONSOR/MONITOR'S ACRONYM(S)
	11. SPONSOR/MONITOR'S REPORT NUMBER(S)

12. DISTRIBUTION/AVAILABILITY STATEMENT
Approved for public release, distribution unlimited

13. SUPPLEMENTARY NOTES
See also ADM002075., The original document contains color images.

14. ABSTRACT

15. SUBJECT TERMS

16. SECURITY CLASSIFICATION OF:			17. LIMITATION OF ABSTRACT	18. NUMBER OF PAGES	19a. NAME OF RESPONSIBLE PERSON
a. REPORT	b. ABSTRACT	c. THIS PAGE			
unclassified	**unclassified**	**unclassified**	**UU**	**7**	

Standard Form 298 (Rev. 8-98)
Prescribed by ANSI Std Z39-18

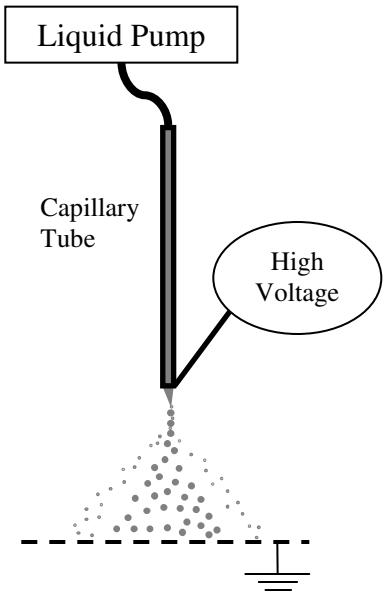

Figure 1. Fundamental electrospray configuration.

extractor electrode and a grounded plane. The ring extractor and ground plane act to minimize space charge effects that eventually lead to the shielding of some nozzles from the voltage source.

The assembled atomizer functions by connecting the nozzle array and the electrode to a voltage source, creating a strong electrical potential difference between the two. A Taylor-cone forms at the tip of each nozzle from the electro hydrodynamic (EHD) and capillary forces. Exceeding a threshold applied electric field strength will cause small charged droplets to be ejected from the cone tip and accelerate through the opening in the ring extractor. The surrounding environment will typically have a fluid removal capability, such as

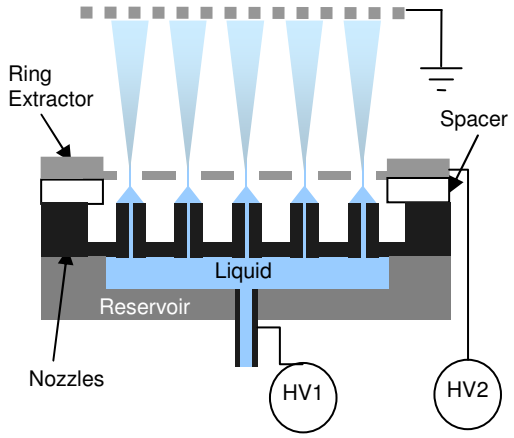

Figure 2. Schematic drawing of a multiplexed electrospray device and the setup for testing. The grounded screen acts to draw the fuel droplets away from the device in place of a combustor or air flow.

combustion, an air-stream, or an additional electrode, to prevent the droplet from returning to the ring extractor electrode. In this work the grounded electrode is used during experimentation to pull the charged fluid droplets away from the ring extractor and prevent puddling and space charge effects.

The droplet ejection will occur continuously from each nozzle as long as the voltages stay above threshold. Because the droplets are charged, they will tend to repel one another by Coulombic repulsion and create a mono-dispersed droplet cloud. Deng et al. provided a study into the various configurations and discussions that lead to the design of the integrated nozzle and ring extractor shown in Figure 3 [Deng et al. 2006 and Deng, Waits et al. 2006].

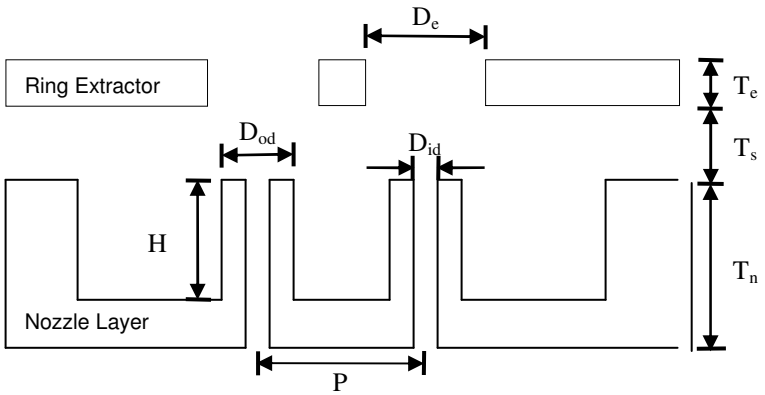

Extractor Layer	Nozzle Layer
D_e = 400 µm	D_{od} = 210 µm
T_e = 200 µm	D_{id} = 60 µm
	H = 460 µm
Spacer Layer	P = 675 µm
T_s = 400 µm	T_n = 775 µm

Figure 3. Integrated multiplexed electrospray design and dimensions

3. FABRICATION

The integrated multiplexed electrospray consists of three layers: 1) the ring extractor which acts as an electrode to pull away the droplets from the nozzle as well as to shield the nozzles from space charge effects; 2) the spacer which acts as a standoff to obtain isolation between the silicon nozzles and the silicon ring extractor and; 3) the nozzles. The ring extractor and nozzle components are fabricated using silicon due to the widely available processes from MEMS fabrication and the semiconductor industry. A Pyrex substrate is chosen for the spacer due to the ease of integration with the silicon components and the high breakdown voltage.

3.1 Ring extractor fabrication

The ring extractor was designed with a thickness of 200µm to allow the droplet cloud to diverge without hitting the sidewalls. Initially, a wafer thickness of 200µm was used to fabricate the ring extractor. During the integration step to the other components using anodic bonding (described below in section 3.3) the thin wafer exhibited stress fracturing across the entire wafer. It is unclear at this time as to the cause of the stress fracturing. The problem was avoided, however, by using a more conventional wafer thickness of 440µm and thinning the array regions to 200µm. Ring extractors fabricated in this fashion are able to survive the bonding process.

Figure 4 shows the fabrication flow for the altered silicon ring extractor. The starting wafer is a 440µm thick 4-inch double-sided polished silicon wafer with a 1µm thermal silicon dioxide grown on the surface. In the first step of the ring extractor fabrication (Figure 4a) photoresist is patterned and the silicon dioxide layer is etched (Figure 4b) using reactive ion etching (RIE) to form the masking layer for the holes on the backside of the silicon. A second photolithography step (Figure 4c) is carried out using front-to-back photolithography along with RIE (Figure 4d) to pattern the large thinning area into the front-side silicon dioxide. The backside holes are etched using deep reactive ion etching (DRIE) to a depth greater than the 200µm desired thickness (Figure 4e). The wafer is then flipped over and attached to a carrier wafer using thermal grease and thinning is performed using a second DRIE step (Figure 4f). Afterwards, the ring extractor is released from the carrier wafer using Acetone and the silicon dioxide is stripped using an HF:H_2O solution (Figure 4g).

3.2 Silicon nozzle fabrication

Figure 5 shows the fabrication flow for the silicon nozzle wafer. The starting wafer is a 4-inch 775µm thick silicon wafer with a 1µm silicon dioxide thermally grown on both sides. The thicker wafer is necessary to allow

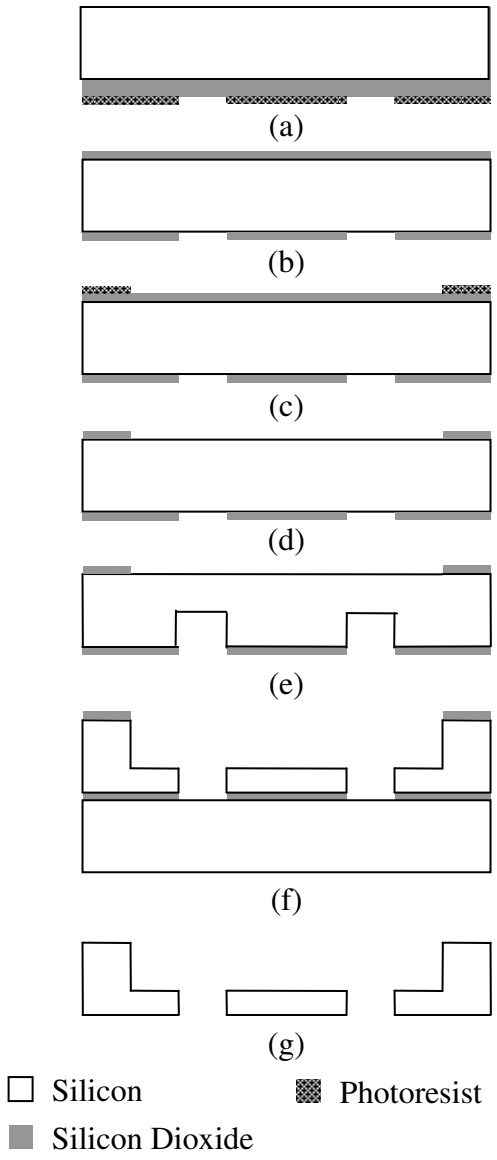

Figure 4. Fabrication flow for the ring extractor.

for the 460µm tall nozzles to have sufficient mechanical support during further processing and component testing. Photolithography and RIE are used to pattern the silicon dioxide on the backside of the wafer (Figure 5a and 5b). The photoresist is removed and the silicon dioxide is used as a masking layer in DRIE to form the through holes to the nozzles (Figure 5c). The nozzles are then patterned on the front-side of the wafer using front-to-back photolithography and etched via RIE into the silicon dioxide with the photoresist remaining afterwards (Figure 5d and 5e). The wafer is then attached to a carrier wafer using thermal grease. With the photoresist and silicon dioxide as a dual-layer mask, the exposed silicon is etched via DRIE to form the nozzles with a height of 460µm (Figure 5f). The wafer is then released from the carrier wafer using Acetone and the silicon dioxide stripped in an HF:H_2O solution (Figure 5g).

The DRIE of the topside silicon nozzles using a standard "High Etch Rate Process" shown in Table 1 produced highly angled sidewalls, which caused many of the nozzle walls to collapse during post-DRIE handling of the wafer. This occurs because large open areas surrounding the nozzles allow ions to sputter the sidewall at high incidence angles resulting in a negative profiled sidewall. Figure 6a shows an SEM profile of a silicon nozzle etched using a standard, high etch rate process. The nozzle exhibits a sidewall taper of greater than 6° causing the wall thickness to disappear if etched to a depth of 460µm.

Process Parameter	High Etch Rate Process		Modified Process	
	Dep.	Etch	Dep.	Etch
Step Time (sec)	4	6	5	5.5
Chamber Pressure (mTorr)	20	20	20	25
Electrode Power (W)	1	16	1	10.5
Coil Power (W)	850	850	850	850
SF_6 (sccm)	0	100	0	100
C_4F_8 (sccm)	70	0	70	0
Ar (sccm)	40	40	40	40

Table 1. DRIE Etch Parameters

A new process was developed to allow for 90° sidewall profiles (Figure 6b). This process focused on reducing the physical sputtering mechanism during the etching step so the passivation layer would remain on the sidewall of the nozzle longer allowing more anisotropy. The DRIE process achieved nearly 90° sidewalls by reducing the electrode power to 10W and the SF_6 flow rate to 60sccm as well as increasing the chamber pressure to 25mTorr. Reducing the electrode power and the SF_6 flow rate decreases the energy of the ions bombarding the wafer surface, thereby, reducing the amount of sputtering taking place. The increased chamber pressure reduces the number of ions with an incidence angle great enough to bombard the sidewall of the nozzle and allow the passivation layer on the sidewall to survive long enough through the etching step.

The new process, however, reduces the ability to remove the passivation layer during the deposition phase of the DRIE cycle. For very deep etches, such as the one reported here, insufficient passivation removal can result in the formation of black silicon (the unwanted polymer acts to "micro-mask" the etching). In this case, black silicon began to appear after ~300µm. A compromise between ion bombardment minimization and sufficient polymer removal had to be obtained to achieve full nozzle height. The resulting "Modified Process" shown in Table 1 does not produce a perfect 90° sidewall. Instead, a slight negative taper still exists, but is reduced to a point that the nozzles are mechanically stable. Etch

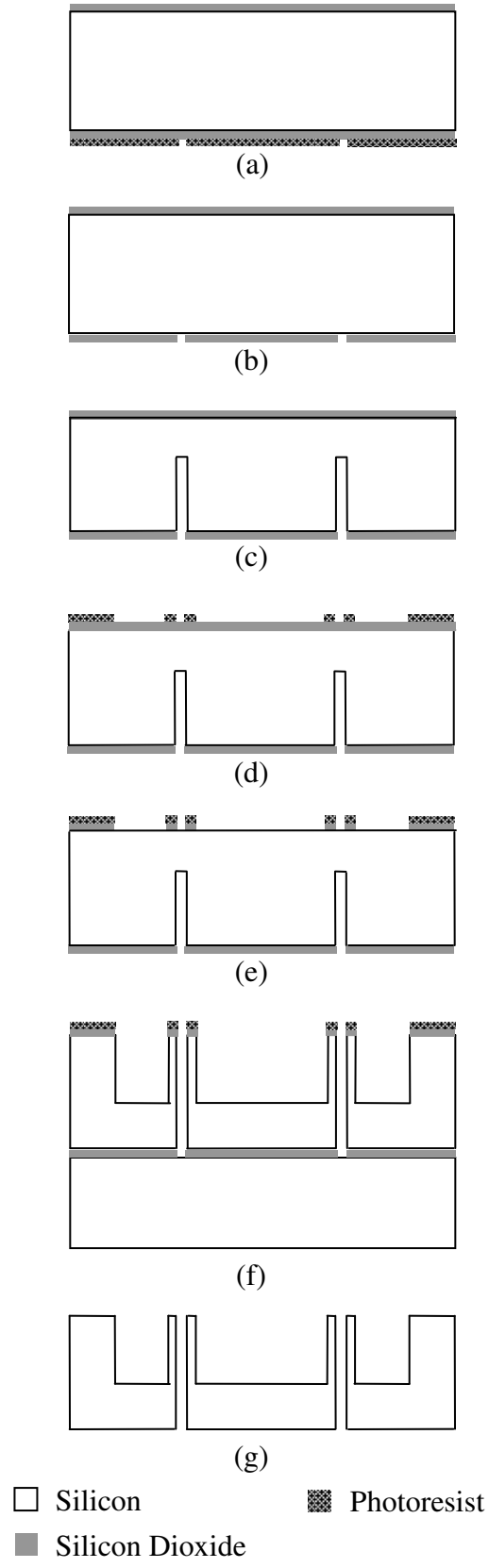

Figure 5. Fabrication flow for the nozzle layer.

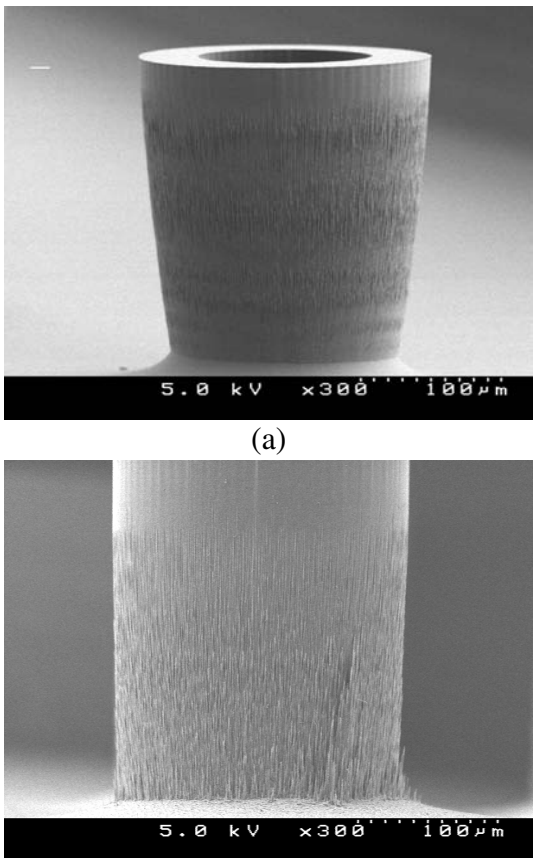

Figure 6. SEM micrograph showing in (a) a nozzle etched using a conventional high etch rate recipe resulting in severely tapered sidewalls and (b) a nozzle etched using the modified process resulting in straight sidewalls.

depths up to 520µm were achieved with the modified process without significant black silicon occurring.

3.3 Component Integration

Integration of the ring extractor and nozzle layers is accomplished using anodic bonding of a 400µm thick Pyrex wafer between the two silicon layers [Despont, 1996] described in sections 3.1 and 3.2. In this case, precision bond aligning can be performed to within 5µm allowing for even further scaling of the nozzles and the ring extractor. Previously, Deng et al. manually aligned individual die using glass frits, limiting the alignment accuracy to ~50µm, thereby limiting further scaling of the device required to achieve higher total flow rates.

Figure 7 shows the bonding procedure for integrating the component wafers. The Pyrex wafer is bonded to the thicker nozzle wafer with an anodic bond process using a 1kV potential across the wafer stack at 300°C and 1Bar of force (Figure 7a). The voltage bias is removed before the current falls below 10% of the initial current. This ensures that enough of the mobile Na^+ ions contained within the glass remain for a second bond. This may reduce the bond strength, but it is believed to be sufficient for the current applications. The ring extractor is then aligned to the bonded stack using a Karl Suss BA-6 bond aligner allowing for ~5µm alignment tolerance (Figure 7b). The same bonding process from the first bond is used to bond the ring extractor to the Pyrex/nozzle stack, although this time allowing the current to saturate. The stack is then put into a 49% HF solution for 85 minutes, etching through the Pyrex wafer using the silicon wafers as the etch masks (Figure 7c). Figure 8 is an SEM picture showing the cross-section of a bonded stack after the Pyrex was etched.

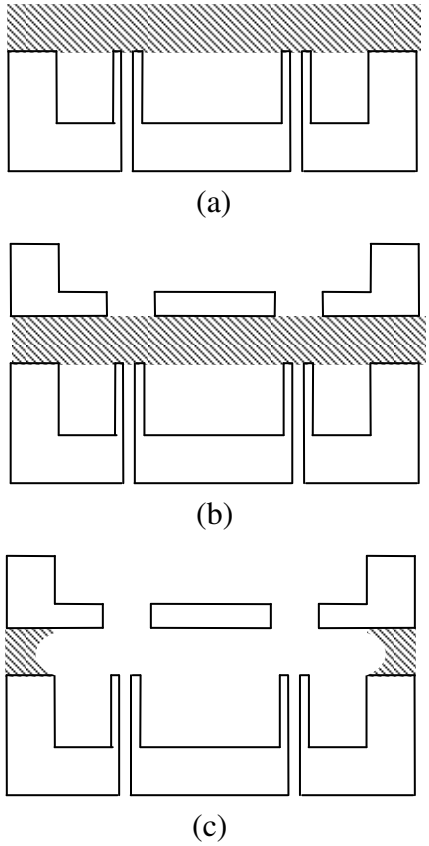

Figure 7. Fabrication flow for the integration of the ring extractor and nozzle silicon layers by sandwiching a Pyrex spacing in-between using aligned anodic bonding.

4. RESULTS AND DISCUSSION

The testing of an integrated device was performed at Yale University of which the process can be found in Deng et al. 2006a and the results along with discussion

can be found in Deng et al. 2006b. The results were taken from a 91-nozzle array using ethanol and 1.8kV applied between the ring extractor and the nozzle wafer. Every nozzle turned on with an average flow rate of 0.2 cc/hour, which is the minimum required to operate the electrospray in cone-jet mode. The droplet diameter was 11μm with a relative standard deviation (RSD) of 2.5%. The total flow rate of the 91-nozzle array was ~20cc/hour, which corresponds to ~20Watts of power in a combustor.

A residual voltage on the order of 100mV between the ring extractor and the nozzle wafer has been recorded for up to an hour after the operating 1.8kV is turned off. Initial thoughts are that the Na^+ contained in the Pyrex glass causes the capacitive like wafer stack to have a very large time constant. Na^+ ions are mobile at elevated temperatures causing the Pyrex layer to be conductive, which is a critical premise to successful anodic bonding. Despite the fact the experiments are conducted at room temperature, the Na^+ ions may still be weakly mobile, affecting the turn-off behavior. Investigations are still being conducted on the effects of the the Na^+ in the glass during the operation of the device.

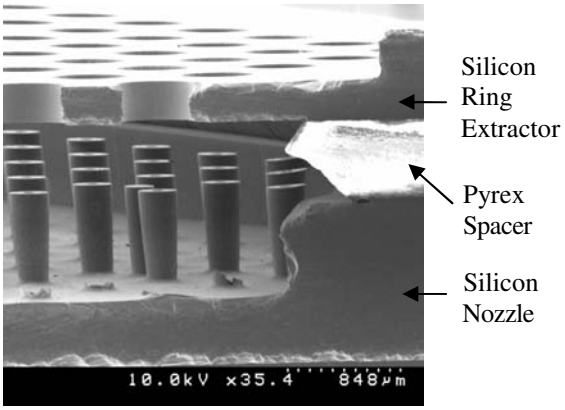

Figure 8. SEM micrograph showing the bonded extractor, spacer, and silicon nozzles using a double sided-anodic bonding process. The missing nozzles were broken off during the cross-sectioning process.

5. CONCLUSIONS

The performance of the integrated electrospray compares favorably with the manually assembled components. Implementing a batch microfabrication process allows for further scaling of the device to increase the nozzle density for higher device flow rates. In addition, further scaling of the device will also decrease the operating voltage requirements, resulting in a very low power device with levels in the sub-mW range for a ~20W combustor device.

References

Bocanegra, R.,Galán, D., Márquez, M., Loscertales, I.G., and Barrero, A., 2005: Multiple electrosprays emitted from an array of holes, *Journal of Aerosol Science*, **36**, pp. 1387-1399.

Deng, W., Klemic, J.F., Li, X., Reed, M.A., and Gomez, A., 2006a: Increase of electrospray throughput using multiplexed microfabricated sources for the scalable generation of monodispersed droplets, *Journal of Aerosol Science,* **37**, pp. 696-714.

Deng, W., Waits, C.M., Jankowski, N., Geil, B. and Gomez, A., 2006b: Optimization of Multiplexed Microfabricated Electrospray Sources to Increase the Flow Rate of Monodispersed Droplets. To be presented at the 7th International Aerosol Conference, St. Paul Minnesota.

Despont, M., Gross, H., Arrouy, F., Stebler, C., Staufer, U., 1996: Fabrication of a silicon-Pyrex-silicon stack by a.c. anodic bonding, *Sensors and Actuators A*, **55**, pp. 219-224.

Epstein, A.H. and coauthors, 1997: Power MEMS and microengines. Proceeding of the 9th International Conference on Solid-State Sensors and Actuators, Chicago, IL., pp. 753-756.

Fréchette, L. G., Lee, C., Arsian, S. and Liu, Y.-C., 2003: Preliminary Design of a MEMS Steam Turbine Power Plant-on-a-chip. Proceeding of the 3rd International Workshop on Micro & Nano Technology for Power Generation & Energy Conversion (Power MEMS'03), Makuhari, Japan, pp. 1-4.

Fu, K. , Knoblock, A. , Martinez, F. , Walther, D.C. Fernandez-Pello, A.C., Pisano, A.P., and Liepmann, D., 2001: Design and Fabrication of a Silicon-Based MEMS Rotary Engine. Proceeding of the ASME 2001 International Mechanical Engineering Congress and Exposition (IMECE), New York, NY.

Groshenry, C., 1995: Preliminary study of micro-gas turbine engine, *S.M. Thesis*, Massachusetts Institute of Technology, Cambridge, Massachusetts.

Kyritsis, D., Guerrero-Arias, I., Roychoudhury, S. and Gomez, A., 2002: Mesoscale Power Generation by a Catalytic Combustor Using Electrosprayed Liquid Hydrocarbons. Proceeding of the Combustion Institute, **20**, pp. 965-972.

Muler, N. and Fréchette, L.G., 2002: Performance Analysis of Brayton and Rankine Cycle Microsystems for Portable Power Generation. Proceeding of the ASME International Mechanical Engineering Congress and Exposition (IMECE), New Orleans, LA, pp. 1-10.

Tang, K., Lin, T., Matson, D.W., Kim, T., Smith, R.D., 2001: Generation of multiple electrosprays using microfabricated emitter arrays for improved mass spectrometric sensitivity, *Analytical Chemistry*, **73**, pp. 1658-1663.

Walther, D. C. and Pisano, A. P. , 2003: MEMS Rotary Engine Power System: Project Overview and Recent Research Results. Proceeding of the 4th International Symponsium on MEMS and Nanotechnology, Charlotte, NC., pp. 227-234.

Zeleny, J., 1914: The Electrical Discharge from liquid points, and a Hydrostatic Method of Mearuring the Electric Intensity at their Surfaces, *The Physical Review*, **3**, pp. 69-91.